

Supporting Information

Improved capacitive performances and electrocatalytic reduction activity by regulating the bonding interaction between Zn-bistriazole-pyrazine/pyridine units and diverse Anderson-type polyoxometalates

Ju-Ju Liang, Yu-Chun Lin, Zhi-Han Chang, Xiu-Li Wang*

College of Chemistry and Materials Engineering, Bohai University, Professional Technology Innovation Center of Liaoning Province for Conversion Materials of Solar Cell, Jinzhou 121013, P. R. China

Materials and methods

Ligands and other reagents were purchased from commercial sources and used directly without purification. FT-IR spectra were determined on a Varian 640 FT-IR spectrometer through KBr pellets in the range of 500–4000 cm^{-1} . Powder X-ray diffraction (PXRD) patterns were collected by a D/teX Ultra diffractometer with Cu $K\alpha$ radiation ($\lambda=1.5418 \text{ \AA}$). The Electrocatalytic reduction and sensing performances experiments were carried out by CHI760E electrochemical workstation with Ag/AgCl as the reference electrode, platinum wire as the auxiliary electrode. Complexes **1–3** modified carbon paste electrodes as working electrode, designed a traditional three electrode system. The capacitance performances of complexes **1–3** was tested on a CHI760 electrochemical workstation. The glassy carbon electrodes (GCEs) modified by the complexes were used as working electrodes, the graphite rod and saturated calomel electrode (SCE) were assigned as the counter and reference electrodes, respectively.

X-ray crystallography

Crystal data of complexes **1–3** were collected on Bruker SMART APEXII with Mo $K\alpha$ radiation ($\lambda=0.71073 \text{ \AA}$) system. The structure of **1–3** is solved by direct method and refined by full matrix least squares on F^2 using Olex2 software.

Preparation of $\text{Cs}_3[\text{CrMo}_6\text{H}_6\text{O}_{24}]\cdot 8\text{H}_2\text{O}$ and $\text{Cs}_6[\text{TeMo}_6\text{O}_{24}]\cdot 6\text{H}_2\text{O}$ and their glassy carbon electrodes (Cs-CrMo₆, Cs-TeMo₆)

0.1 g $\text{NH}_3[\text{CrMo}_6\text{H}_6\text{O}_{24}]\cdot 8\text{H}_2\text{O}^1$ and 0.1 g $\text{NH}_6[\text{TeMo}_6\text{O}_{24}]\cdot 6\text{H}_2\text{O}^2$ were dissolved

in 10 mL deionized water, respectively, and 2 ml of 1 mol/L CsCl solution was added. The insoluble precipitates obtained were washed with deionized water after sonication for 30 min. The corresponding insoluble salts were obtained by drying in an oven at 80 °C overnight. The insoluble salt-modified glassy carbon electrodes were prepared using the method described in the section of **Preparations of 1–3–GCEs**.

Preparations of 1–3 modified carbon paste electrodes (1–3–CPEs)

The graphite nano-powder (0.1 g) and complexes **1**, **2** or **3** (0.015 g) were accurately weighed and mixed thoroughly with grinding in a mortar for 45 min, and an appropriate amount of paraffin oil was added dropwise to the ground powder and stirred to a paste-like mixture. The above substances were transferred to a glass tube with an inner diameter of 3 mm, compacted with a copper rod, and the electrode surface was polished to smooth with a weighing paper³.

Preparations of 1–3 modified glassy carbon electrodes (1–3–GCEs)

The glassy carbon electrode (GCE) was polished before each experiment with 1, 0.3 and 0.05 mm alumina powder on chamois leather, respectively, rinsed fully with deionized water between each polishing step. In order to prepare the working electrode, the mixture of 5 mg crystal and 25 mg activated carbon was fully ground in a mortar. Then the above mixture was sonicated in a mixed solvent of water (300 μ L) and ethanol (100 μ L) for 1 hour to form a uniform turbid liquid. 10 μ L of well dispersed slurry was dropped onto the GCE with a diameter of 4 mm and dried for 2 hours at room temperature to form a uniform thin film. Finally, 5 μ L of Nafion solution was dropped onto the GCE surface, and the electrode was dried at room temperature⁴.

Table S1 Partial bond lengths and bond angles of complex **1**

1			
Zn1-N1	2.194(3)	Zn1-N2	2.178(3)
Zn1-O1W	2.114(3)	Zn1-O2W	2.064(3)
Zn1-O3W	2.058(3)	Zn1-O4W	2.112(3)
O1W-Zn1-N1	90.99(12)	O1W-Zn1-N2	93.94(12)
O2W-Zn1-O1W	91.79(14)	O2W-Zn1-N1	89.13(13)
O2W-Zn1-O4W	87.45(15)	O2W-Zn1-N2	165.04(12)
O3W-Zn1-N2	98.83(12)	O3W-Zn1-O1W	87.05(13)
O3W-Zn1-N1	175.26(13)	O3W-Zn1-O4W	89.42(14)
O3W-Zn1-O2W	95.25(13)	N2-Zn1-N1	76.98(12)

O4W-Zn1-N2	87.67(13)	O4W-Zn1-O1W	176.30(13)
O4W-Zn1-N1	92.62(13)		

Symmetrycodes: ¹1-X,+Y,3/2-Z

Table S2 Partial bond lengths and bond angles of complex **2**

2			
Zn1-O1	2.133(2)	Zn1-O1W	2.134(2)
Zn1-O2W	2.069(2)	Zn1-N1	2.138(3)
Zn1-N2	2.127(3)	Zn1-O3W	2.113(3)
O1-Zn1-O1W	85.79(9)	O1-Zn1-N1	174.98(9)
O1W-Zn1-N1	94.52(9)	O2W-Zn1-O1	90.84(10)
O2W-Zn1-O1W	84.16(10)	O2W-Zn1-N1	94.18(10)
O2W-Zn1-N2	170.18(10)	O2W-Zn1-O3W	87.02(13)
N2-Zn1-O1	97.23(9)	N2-Zn1-O1W	90.83(10)
N2-Zn1-N1	77.76(10)	O3W-Zn1-O1	87.72(11)
O3W-Zn1-O1W	168.96(12)	O3W-Zn1-N1	92.73(12)
O4-Mo1-O12	71.67(8)	O3W-Zn1-N2	98.85(13)

Symmetrycodes:¹2-X,1-Y,1-Z

Table S3 Partial bond lengths and bond angles of complex **3**

3			
Zn1-N1	2.174(3)	Zn1-N2	2.176(3)
Zn1-O1	1.994(4)	Zn1-O2	2.194(4)
Zn1-O1W	2.076(5)	Zn1-O2W	2.127(5)
Zn2-O1	1.871(5)	Zn2-O3	2.314(4)
Zn2-N3	2.022(5)	Zn2-O11 ³	2.255(4)
Zn2-O3W	1.954(5)	Zn3-N4	2.050(5)
Zn3-N5 ²	2.173(5)	Zn3-N6 ²	2.090(5)
Zn3-O4W	2.050(4)	Zn3-O5W	1.997(5)
O4W-Zn3-N4	88.29(19)	O4W-Zn3-N5 ²	155.96(18)
O4W-Zn3-N6 ²	93.12(18)	N4-Zn3-N5 ²	94.31(18)
N4-Zn3-N6 ²	159.5(2)	O5W-Zn3-O4W	104.6(2)
O5W-Zn3-N4	98.4(2)	O5W-Zn3-N5 ²	98.6(2)
O5W-Zn3-N6 ²	101.0(2)	N6 ² -Zn3-N5 ²	76.37(19)
O1W-Zn1-O2	91.07(18)	O1W-Zn1-O2W	87.8(2)

O1W-Zn1-N1	91.62(19)	O1W-Zn1-N2	169.34(19)
O2W-Zn1-O2	175.44(18)	O2W-Zn1-N1	90.81(18)
O2W-Zn1-N2	92.11(18)	O1-Zn1-O2	83.78(18)
O1-Zn1-O1W	90.3(2)	O1-Zn1-O2W	100.62(19)
O1-Zn1-N1	168.48(19)	O1-Zn1-N2	100.22(19)
N1-Zn1-O2	84.82(17)	N1-Zn1-N2	77.71(18)
N2-Zn1-O2	88.21(17)	O11 ³ -Zn2-O3	163.71(16)
O1-Zn2-O3	100.47(18)	O1-Zn2-O11 ³	91.43(18)
O1-Zn2-O3W	113.7(3)	O1-Zn2-N3	114.3(2)
O3W-Zn2-O3	82.38(18)	O3W-Zn2-O11 ³	82.66(18)
O3W-Zn2-N3	131.9(3)	N3-Zn2-O3	91.00(18)
N3-Zn2-O113	94.21(18)		

Symmetrycodes: ¹1-X,1-Y,1-Z; ²2-X,1-Y,2-Z; ³2-X,1-Y,1-Z

Table S4 Hydrogen bonds of complex **1**(Å).

D-H...A	D-H	H...A	D...A	D-H...A
O(1W)-H(1WA)···O(1)	0.85	1.86	2.652(4)	155
O(4W)-H(4WA)···O(4)	0.85	1.85	2.670(4)	162

Table S5 Hydrogen bonds of complex **2**(Å).

D-H...A	D-H	H...A	D...A	D-H...A
O(1W)-H(1WB)···O(6)	0.85	1.89	2.735(4)	173
O(2W)-H(2WB)···O(10)	0.85	1.97	2.810(3)	167

Infrared spectroscopic analysis of complexes 1–3

Fig.S1 shows the IR spectra of **1–3**. The characteristic absorption peaks of 644, 914, 1050 cm⁻¹ for **1**, 605,815,966 cm⁻¹ for **2** and 605, 914, 996 cm⁻¹ for **3** are attributed to the vibration of $\nu(\text{Mo}=\text{O}_t)$ and $\nu(\text{Mo}-\text{O}-\text{Mo})^5$ in complexes **1–3**. And other peaks can be attributed to the presence of ligands⁶. In the three complexes, the characteristic peak of hydroxyl group⁷ of water molecule can be observed near 3000~3400 cm⁻¹.

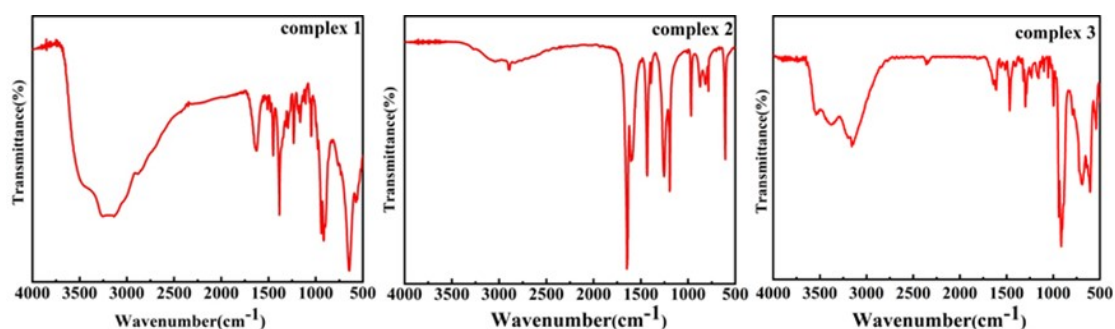


Fig.S1 IR spectra of complexes 1–3.

X-ray powder diffraction analysis of complexes 1–3

The powder X-ray diffraction spectra of complexes 1–3 were analyzed at room temperature. It can be observed from Fig.S2 that the experimental peak positions of the synthesized complexes 1–3 are consistent with the simulated ones, which proves that the phase purity of the three complexes is high⁸.

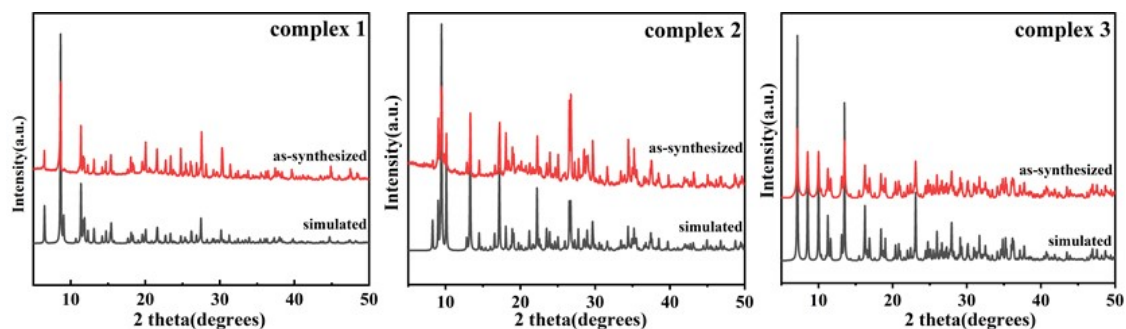


Fig.S2 X-ray powder diffraction patterns of complexes 1–3.

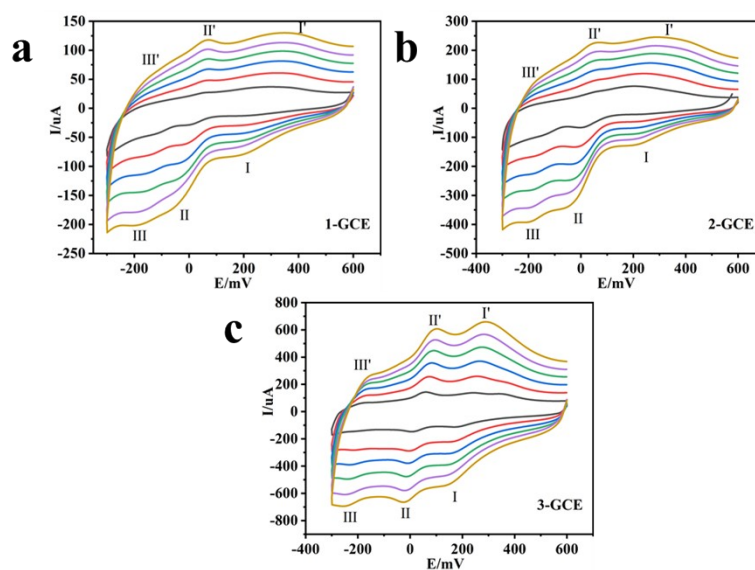


Fig.S3 The CV curves of 1–3–GCEs at 5, 10, 15, 20, 25 and 30mV s⁻¹.

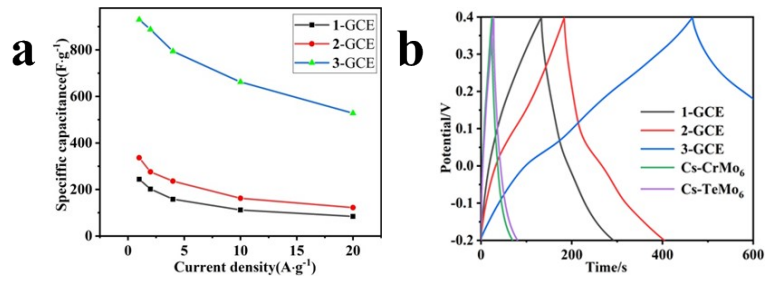


Fig. S4 (a) The specific capacitance values of 1–3–GCEs; (b) GCD curves of Cs-CrMo₆ and Cs-TeMo₆ and comparative plots of complexes 1-3 with different coordination modes introduced.

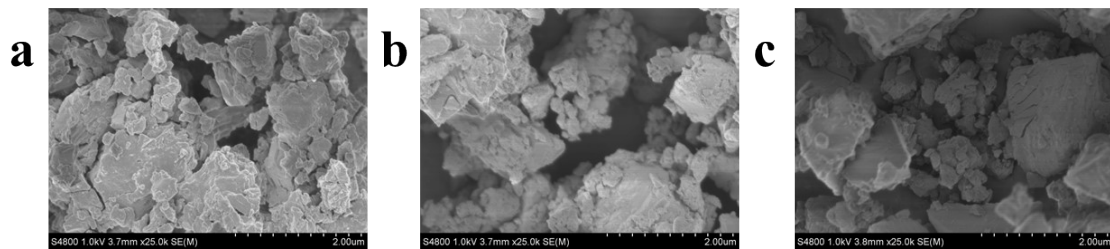


Fig.S5 SEM images with particle size analysis of the POM material on the electrode.

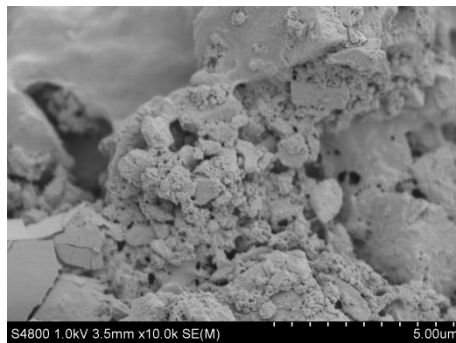


Fig. S6. SEM image after 5000 cycling.

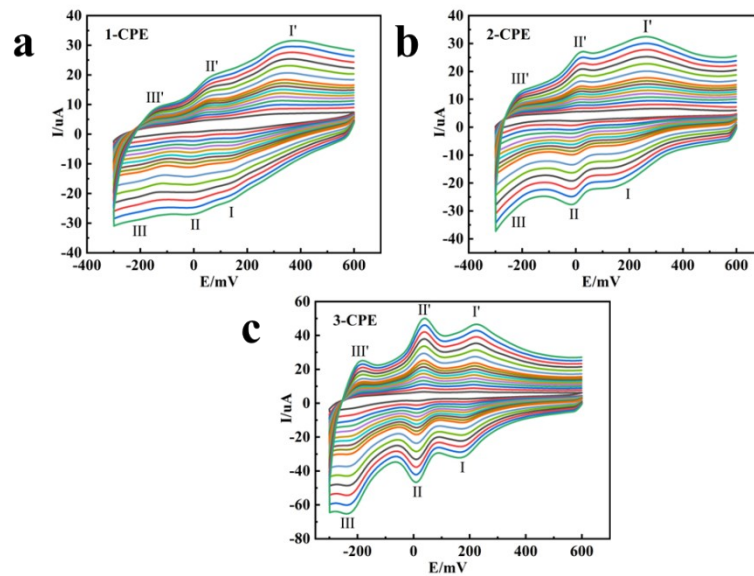


Fig. S7 The CV curves of 1–3–CPEs at different scan rates.

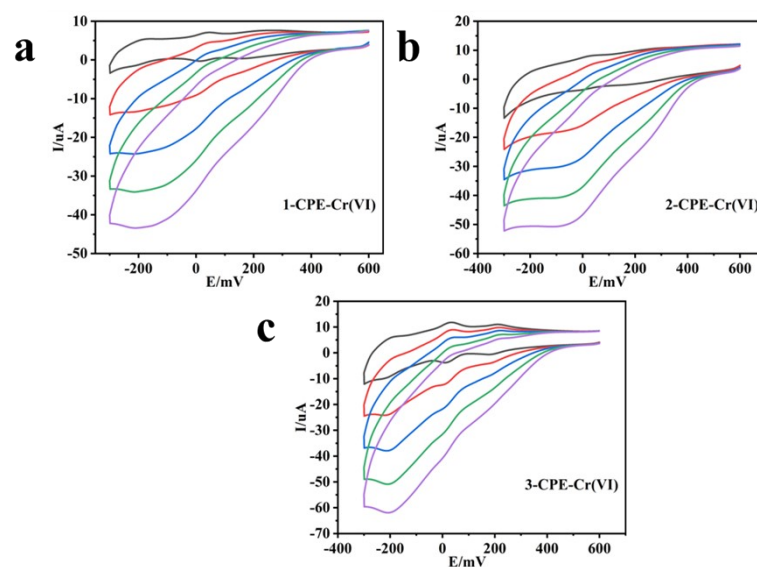


Fig. S8 The CV curves of **1–3**–CPEs in solutions with different concentrations of Cr (VI) at a scan rate of 60 mV s^{-1} .

1. X. Wang, J. Sun, H. Lin, Z. Chang, G. Liu, X. Wang, *RSC Advances*, 2016, **6**, 110583-110591.
2. C. I. Cabello, Botto, I. L., Cabrerizo, F., González, M. G., & Thomas, H. J., *Adsorption Science & Technology*, 2000, **18(7)**, 591-608.
3. J.-J. Lu, J.-J. Liang, H.-Y. Lin, Q.-Q. Liu, Z.-W. Cui, X.-L. Wang, *CrystEngComm*, 2022, **24**, 3921-3927.
4. Y. Chen, Z. Chang, Y. Zhang, K. Chen, X. Wang, *Inorg Chem*, 2022, **61**, 16020-16027.
5. D. Xiao, Y. Hou, E. Wang, S. Wang, Y. Li, L. Xu, C. Hu, *Inorganica Chimica Acta*, 2004, **357**, 2525-2531.
6. X. Wang, X. Bai, H. Lin, J. Sun, G. Liu, X. Wang, *CrystEngComm*, 2018, **20**, 6438-6448.
7. J. Sárkány, *Applied Catalysis A*, 1999, **188**, 369.
8. Q. Q. Liu, X. L. Wang, H. Y. Lin, Z. H. Chang, Y. C. Zhang, Y. Tian, J. J. Lu, L. Yu, *Dalton Trans*, 2021, **50**, 9450-9456.